

Simulated causal subwavelength focusing by a negative refractive index slab

Steven A. Cummer^{a)}

Department of Electrical and Computer Engineering, Duke University, Durham, North Carolina 27708

(Received 16 October 2002; accepted 16 December 2002)

Subwavelength electromagnetic focusing by a negative refractive index slab is shown to occur in a full wave numerical simulation of a causal, physically realizable negative index material. Limitations on the observability of this effect in simulations and experiments are discussed.

© 2003 American Institute of Physics. [DOI: 10.1063/1.1554778]

Pendry¹ showed how normally evanescent electromagnetic waves can exponentially grow in a finite slab of material with an index of refraction $n = -1$. In principle, this can produce perfect focusing, in which the fields at a distant location are an exact replica of the source, including subwavelength features. This phenomenon is of more than academic interest because of the constructability of electromagnetic materials with a negative index of refraction.² The potential applications of this effect are numerous and span many different fields.

The existence of this solution is surprising and not intuitive. Reports have questioned the correctness of the perfect focus solution³ and the realizability of this solution from a causal excitation.^{4,5} Moreover, a causal, full wave electromagnetic simulation of focusing by a negative index slab did not appear to show evidence of subwavelength focusing.⁶

We report here a finite-difference simulation and analysis that show that nonpropagating wave numbers do grow in a finite slab of physically realizable negative index material from a causal excitation and, with the proper geometry, such a system produces an image with subwavelength resolution. True perfect focusing is not observed for reasons of solution sensitivity to the precise $n = -1$ condition that have been analytically demonstrated by Smith *et al.*⁷ But subwavelength focusing, in which some but not all evanescent wave numbers are restored and the image contains subwavelength information, is clearly seen in the reported simulation in the manner predicted analytically.

We perform a time-domain finite-difference simulation of the Maxwell equations for the predicted perfect focusing geometry. Without loss of generality, we assume two-dimensional ($\partial/\partial y = 0$) transverse magnetic (TM) ($E_y, H_x, H_z \neq 0$) fields in a domain with material properties varying only in the z direction. E_y is specified completely on the plane $z=0$ as a sinusoidal line source $E_y(x,0) = \delta(x)\sin(2\pi \times 10^{10}t)f(t)$, where $f(t)$ is a step function that turns on smoothly in about 30 wave periods. The smooth turn on helps the fields reach their steady state as quickly as possible by minimizing the excitation bandwidth. Free space is present for $0 < z < 6.52$ mm and $z > 19.56$ mm. Between $z = 6.52$ and $z = 19.56$ mm is a slab of material with relative permittivity and permeability

$$\epsilon_r(\omega) = \mu_r(\omega) = 1 - \frac{\omega_p^2}{\omega^2}. \quad (1)$$

This material has both electric and magnetic plasma responses and we thus refer to it as a two cutoff material. The electric and magnetic plasma frequencies are chosen to give an index of refraction of $n = -1$ at the 10 GHz source frequency, namely $\omega_p = 2\sqrt{2}\pi \times 10^{10} \text{ s}^{-1}$. Small loss (electric and magnetic plasma collision frequency $\nu = 10^7 \text{ s}^{-1}$) is also added to ensure the solution reaches a steady state in finite time. These parameters give a relative permittivity and permeability of $-1 - 0.0006j$ at 10 GHz. This two cutoff material is the simplest way to simulate a material response that produces a frequency band of negative refractive index. Note that the source is quite close (0.22λ) to the two cutoff material slab.

We use the standard second-order leapfrog method⁸ to simulate the electromagnetic fields in this domain. The electric and magnetic plasma responses are easily included through additional equations for electric and magnetic current using the differencing scheme of Young.⁹ This method is nearly identical to that used by Ziolkowski and Heyman.⁶ We find that shifting the x component of the magnetic current to the E_y sampling points by spatial averaging improves the steady-state agreement between theory and simulation. We, therefore, use this averaging in the results presented, although subwavelength focusing can be simulated without this averaging. The simulation uses a time step of $\Delta t = 0.75$ ps, a spatial step of $\Delta x = 0.326$ mm, and a primary computational domain of 600 by 100 cells. The source point is placed at gridpoint (300,1). The fields at the $z=0$ boundary are fully specified by the hard source, and the perfectly matched layer absorbing boundary condition¹⁰ is used to simulate an open boundary at $z = 32.6$ mm (6.52 mm beyond the second focus plane). Because of the difficulty in designing absorbing boundary conditions in the two cutoff material, we use periodic boundary conditions on the constant x edges of the computational domain. This makes the effective source a series of line sources and does not hinder the ability to simulate the perfect focusing effect.

The source is turned on and the simulation is run for 10^5 time steps (750 wave periods) to reach the sinusoidal steady state. Pendry¹ showed that, without loss, this problem reaches a steady state in which the fields at $z = 13.04$ mm and

^{a)}Electronic mail: cummer@ee.duke.edu

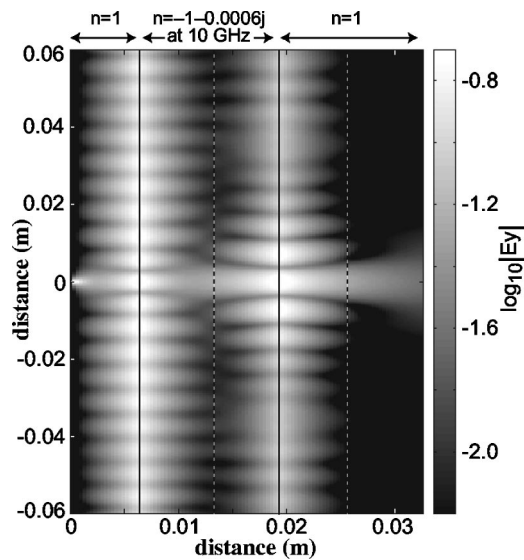


FIG. 1. Image of the sinusoidal steady state $|E_y|$ reached by the simulation. The solid lines show the material boundaries, and the dashed lines are the theoretical perfect focus planes.

$z = 26.08$ mm (the perfect foci) are perfect replicas of the fields at $z = 0$. In practice, however, the sensitivity of the solution to medium parameters, including the loss added to make the solution reach a steady state in a manageable time, will prevent perfect focusing.⁷ Nevertheless, subwavelength focusing is observed in the simulation. Figure 1 shows the spatial distribution of $|E_y|$ after the solution reaches steady state. The transverse variation of the focus plane fields (discussed in detail later) appears to be roughly a sinc function $[\sin(x)/x]$. This is expected if a finite range of transverse wave numbers are able to reach the focusing plane at full amplitude and in phase, and does not by itself imply subwavelength focusing.

If the two cutoff slab only restored the phase of propagating waves but not the amplitude of evanescent waves, then the electric field in the second focus plane could contain only sinusoidal features above one wavelength in size because of the evanescent decay of smaller features. The spatial variation of this field in the focus plane, obtained by Fourier transforming the transverse wave number spectrum, would be a sinc function with a main lobe zero-to-zero spacing of one wavelength. This is the one wavelength resolution limit considered by Pendry¹ (one of many possible definitions of the resolution limit) and corresponds to the full width of the field produced by a single point source that can be obtained with infinite aperture traditional optics. This limit is shown by the dashed lines in Fig. 2, in which the wave number spectrum is not perfectly sharp because the near cutoff wave numbers do not fully decay over the relatively short source-to-focal-plan distance considered in this problem.

The field intensity from the full wave simulation in the second focal plane and corresponding wave number spectrum are shown in the solid lines of Fig. 2. The variation is sinelike, but the actual width of the main peak is only 0.41λ , corresponding to focusing 2.4 times smaller than one wavelength. The wave number spectrum of the simulated fields clearly shows that the amplitude of evanescent transverse wave numbers up to 2.5 times the free space wave number ($2.5k_{fs}$) are restored to near unity by the two cutoff slab. The

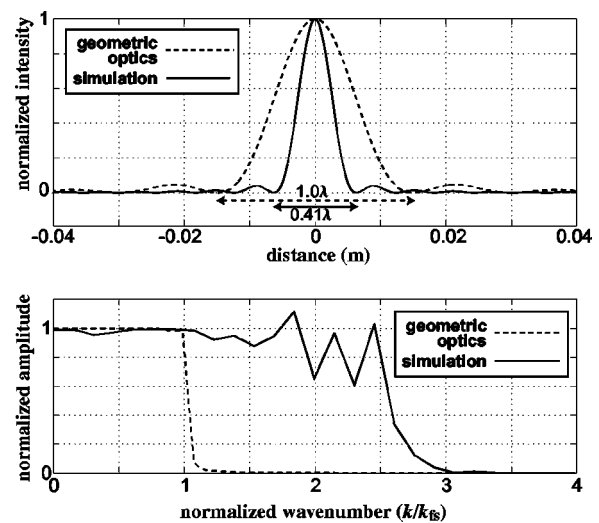


FIG. 2. Top panel: Optics-limited and simulated field intensity in the second focal plane, showing subwavelength focusing from the negative index slab. Bottom panel: Optics-limited and simulated transverse wave number spectrum in the same plane, showing that the amplitude of the evanescent transverse wave numbers ($k/k_{fs} > 1$) is restored by the negative index slab up to a limit of $2.5k_{fs}$.

sharp features in the simulated wave number spectrum beginning near $2k_{fs}$ are likely due to the same small numerical refractive index variations discussed next that make subwavelength focusing hard to simulate in the first place, and they do not influence the conclusions of this work. We emphasize that these results come from a full wave causal electromagnetic simulation of linear materials, thereby avoiding any issues involving signs, series divergence, or infinite fields that have led to contradictory conclusions about this problem. The observed subwavelength focusing is simply a natural consequence of the material properties.

There are a few reasons why simulating (and achieving in practice) perfect focusing is essentially impossible. We added loss to this simulation so that it reached a steady state in a reasonable amount of time, and the perfect focus solution is degraded by loss.^{3,7} The fields at the perfect focus planes have resonances very near the $n = -1$ frequency that will always be excited by a causal, nonzero bandwidth source. Without loss, these resonances ring indefinitely and the theoretical sinusoidal steady state is never achieved.

Perhaps more importantly, the discrete fields in a finite-difference approximation do not obey exactly the same dispersion relation as the continuous fields do;⁸ they are the same only in the limit as the spatial and temporal sampling intervals tend to zero. Thus, the index of refraction for the discrete fields is slightly different from the index of refraction for continuous fields using the same medium parameters. In most problems, this small difference has little effect on the final solution. However, tiny deviations from $n = -1$ in the negative index slab can severely limit the perfect focusing effect.⁷ The difference between the continuous and discrete fields can always be reduced by more finely discretizing the fields. But the exponential dependence of subwavelength focusing performance on this difference implies only a small improvement in simulated focusing for a large increase in sampling points (and, consequently, computation time).

The expression for resolution enhancement, $R = -\lambda \ln|(1+\mu)/2|/2\pi d$ where d is the negative index material slab width and μ is the permeability of the negative index slab (thus close to $\mu = -1$) [Ref. 7, Eq. (5)], gives a theoretical limit of $R = 2.97$ for the parameters in this simulation (ignoring any effect of the spatial periodicity of n). The simulated resolution enhancement $R_{\text{sim}} = 2.4 - 2.5$ is thus close to the expected limit given the amount of loss added to the negative index slab. Reducing the loss does not improve the simulated resolution enhancement because of the perturbation of the index of refraction for fields on a finite difference grid. It is expected that moving the source closer to the slab and decreasing the slab width, or increasing the fineness of the spatial and temporal discretization and decreasing the loss (thereby moving n closer to its value for continuous fields) will increase the degree of resolution enhancement observable in the simulation, in accordance with theory.⁷

We conclude that subwavelength focusing by negative refractive index slabs, as predicted by Pendry,¹ is a real effect. Despite the limitations highlighted by this simulation and that have demonstrated analytically elsewhere,⁷ subwavelength focusing should be observable in experiment. We

suggest that the difficulties of constructing a negative index material with precisely $n = -1$ at the source frequency are similar to the difficulties of constructing a finite-difference approximation with precisely $n = -1$, and that simulations like this are thus a useful approximation of the degree of subwavelength focusing that may be observed in experiments. Measurements will always be limited in the restoration of evanescent wave number amplitude and thus should look similar to the simulated fields in Fig. 1.

¹J. B. Pendry, Phys. Rev. Lett. **85**, 3966 (2000).

²R. A. Shelby, D. R. Smith, and S. Schultz, Science **292**, 77 (2001).

³N. Garcia and M. Nieto-Vesperinas, Phys. Rev. Lett. **88**, 207403 (2002).

⁴G. W. 't Hooft, Phys. Rev. Lett. **87**, 249701 (2001).

⁵J. M. Williams, Phys. Rev. Lett. **87**, 249703 (2001).

⁶R. W. Ziolkowski and E. Heyman, Phys. Rev. E **64**, 056625 (2001).

⁷D. R. Smith, D. Schurig, M. Rosenbluth, S. Schultz, S. A. Ramakrishna, and J. B. Pendry, Appl. Phys. Lett. **82**, 1506 (2003); following paper.

⁸A. Taflov and S. C. Hagness, *Computational Electrodynamics: The Finite-Difference Time-Domain Method* (Artech House, Norwood, Mass., 2000).

⁹J. L. Young, IEEE Trans. Antennas Propag. **44**, 1283 (1996).

¹⁰J.-P. Berenger, IEEE Trans. Antennas Propag. **50**, 258 (2002).